



Time-to-enhancement at ultrafast breast DCE-MRI: potential imaging biomarker of tumour aggressiveness

Sung Ui Shin^{1,2,3,4} · Nariya Cho^{1,2,3} · Soo-Yeon Kim^{1,2,3} · Su Hyun Lee^{1,2,3} · Jung Min Chang^{1,2,3} · Woo Kyung Moon^{1,2,3}

Received: 19 April 2019 / Revised: 20 January 2020 / Accepted: 30 January 2020 / Published online: 6 March 2020
© European Society of Radiology 2020

Abstract

Objectives This study was conducted in order to investigate whether there is a correlation between the time-to-enhancement (TTE) in ultrafast MRI and histopathological characteristics of breast cancers.

Methods Between January and August 2017, 274 consecutive breast cancer patients (mean age, 53.5 years; range, 25–80 years) who underwent ultrafast MRI and subsequent surgery were included for analysis. Ultrafast MRI scans were acquired using TWIST-VIBE or 4D TRAK-3D TFE sequences. TTE and maximum slope (MS) were derived from the ultrafast MRI. The repeated measures ANOVA, Mann–Whitney *U* test and Kruskal–Wallis *H* test were performed to compare the median TTE, MS and SER according to histologic type, histologic grade, ER/PR/HER2 positivity, level of Ki-67 and tumour subtype. For TTE calculation, intraclass correlation coefficient (ICC) was used to evaluate interobserver variability.

Results The median TTE of invasive cancers was shorter than that of in situ cancers ($p < 0.001$). In invasive cancers, large tumours showed shorter TTE than small tumours ($p = 0.001$). High histologic/nuclear grade cancers had shorter TTE than low to intermediate grade cancers ($p < 0.001$ and $p < 0.001$). HER2-positive cancers showed shorter TTE than HER2-negative cancers ($p = 0.001$). The median TTE of cancers with high Ki-67 was shorter than that of cancers with low Ki-67 ($p < 0.001$). ICC between two readers showed moderate agreement (0.516). No difference was found in the median MS or SER values according to the clinicopathologic features.

Conclusions The median TTE of breast cancer in ultrafast MRI was shorter in invasive or aggressive tumours than in in situ cancer or less aggressive tumours, respectively.

Key Points

- Invasive breast tumours show a shorter TTE in ultrafast DCE-MRI than in situ cancers.
- A shorter TTE in ultrafast DCE-MRI is associated with breast tumours of a large size, high histologic or nuclear grade, PR negativity, HER2 positivity and high Ki-67 level.

Keywords Breast · Neoplasms · Magnetic resonance imaging

Electronic supplementary material The online version of this article (<https://doi.org/10.1007/s00330-020-06693-0>) contains supplementary material, which is available to authorized users.

✉ Nariya Cho
river7774@gmail.com

- ¹ Department of Radiology, Seoul National University Hospital, Seoul, Republic of Korea
- ² Department of Radiology, Seoul National College of Medicine, 101 Daehak-ro, Jongno-gu, Seoul 110-744, Republic of Korea
- ³ Institute of Radiation Medicine, Seoul National University Medical Research Center, Seoul, Republic of Korea
- ⁴ Seoul National University Hospital Healthcare System Gangnam Center, Seoul, Republic of Korea

Abbreviations

DCE	Dynamic contrast-enhanced
ER	Oestrogen receptor
eTHRIVE	Enhanced T1-weighted high-resolution isotropic volume examination
HER2	Human epidermal growth factor receptor (HER)-2
IHC	Immunohistochemistry
MRI	Magnetic resonance imaging
MS	Maximum slope
PR	Progesterone receptor
ROI	Region of interest
SER	Signal enhancement ratio
TFE	Turbo field echo

TRAK	Time-resolved MR angiography with keyhole
TTE	Time-to-enhancement
TWIST	Time-resolved angiography with interleaved stochastic trajectories
VIBE	Volume-interpolated breath-hold examination

Introduction

With the recent advent of fast MRI techniques, breast ultrafast dynamic contrast-enhanced (DCE)-MRI with very high temporal resolution (4 to 7 s) and moderate spatial resolution has become widely available [1, 2]. Ultrafast breast MRI can acquire whole-breast 3D images at multiple time points within 1 min after contrast injection, which is followed by conventional high-spatial resolution DCE-MRI. Thus, ultrafast breast MRI can provide kinetic information at very early time points. Early kinetic information from ultrafast DCE-MRI has been shown to be useful in differentiating benign and malignant breast lesions [3–7]. Time-to-enhancement (TTE), defined as the arrival time of the contrast agent from the aorta to the breast lesion, has been consistently shown to be significantly shorter in breast cancer tissue than in benign lesions [3–6]. A recent study has also suggested that initial enhancement analysis using ultrafast DCE-MRI is notably more useful for differentiating of non-mass enhancements than conventional DCE-MRI [8].

In addition to the differentiation of benign and malignant lesions, kinetic information derived from conventional DCE-MRI has been shown to correlate with tumour invasiveness, tumour grade, proliferation index, tumour aggressiveness [9–12] or disease-free survival [13, 14]. However, to the best of our knowledge, few studies have been published regarding the correlation between the early kinetic parameters derived from ultrafast breast DCE-MRI and the histopathological characteristics of breast cancer [8, 15, 16].

Therefore, the purpose of our study was to investigate whether there was a correlation between the TTE of breast cancer in ultrafast breast DCE-MRI and the histopathological characteristics.

Materials and methods

Patients

This retrospective study was approved by the Institutional Review Board of Seoul National University Hospital and informed consent was waived (IRB No. 1706-019-857). Between January 2017 and August 2017, 483 consecutive women with breast cancer who underwent ultrafast breast DCE-MR examinations and subsequent surgery were retrospectively identified from the Breast Imaging Center database of our institution. Among these patients, we excluded the following patients:

those who had received neoadjuvant chemotherapy ($n = 154$) or excisional biopsy prior to MR examination ($n = 34$), those with no residual tumour at surgical pathology ($n = 3$), those with no identifiable lesion in the breast ($n = 10$), those who experienced technical failure ($n = 7$) and those with incomplete immunohistochemistry (IHC) results ($n = 1$). Technical failure includes motion artefacts ($n = 4$), insufficient fat saturation ($n = 2$) and inadequate timing of the contrast injection ($n = 1$). Finally, 274 women (mean age \pm standard deviation, 53.5 ± 10.9 ; range, 25–80 years) were included in this study. The median interval between MR examination and surgery was 9.0 days (range 1–63 days).

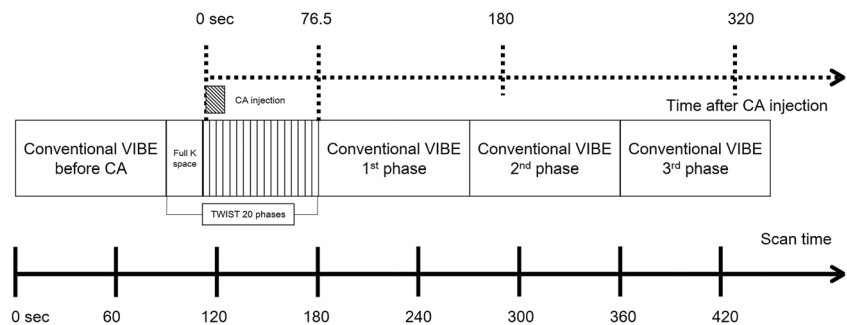
MRI techniques

MR examinations were performed using one of two 3-T MRI scanners (MAGNETOM Skyra, Siemens Healthineers GmbH [$n = 83$] or Ingenia, Philips Healthcare [$n = 191$]) and its own dedicated 16-channel breast coil with the patient in a prone position. Figure 1 shows the ultrafast and conventional DCE-MRI protocol. First, we obtained conventional pre-contrast images and then obtained pre- and post-contrast images with the ultrafast protocol before performing post-contrast conventional MRI. The ultrafast scan yielded a total of 20 phase images with a 3.8- or 4.5-s temporal resolution for MAGNETOM Skyra (Siemens Healthineers GmbH) or Ingenia (Philips Healthcare), respectively. Of the 20 ultrafast phases, the first three were acquired prior to contrast injection, and the following 17 phases were acquired immediately after and during contrast injection. Gadobutrol (Gadovist; Bayer Healthcare) was intravenously injected with a power injector (Spectris Solaris; Medrad Europe) at a dose of 0.1 mmol/kg at a rate of 2 mL/s followed by a 20-mL saline flush. The total acquisition time of the ultrafast scan was 83 or 95 s for MAGNETOM Skyra, Siemens Healthineers GmbH or Ingenia, Philips Healthcare, respectively. The conventional post-contrast acquisition started immediately after the completion of the ultrafast acquisition, which consisted of five phases. A volume-interpolated breath-hold examination (VIBE) or enhanced T1-weighted high-resolution isotropic volume examination (eTHRIVE) sequence with a 90-s temporal resolution was used for conventional DCE-MRI. Time-resolved angiography with interleaved stochastic trajectories (TWIST)-VIBE or a 4D time-resolved MR angiography with keyhole (4D-TRAK)-3D turbo field echo (TFE) sequence was used for the ultrafast DCE-MRI. The detailed acquisition parameters for ultrafast and conventional MRI are summarised in Table 1.

Clinicopathologic information

Clinicopathologic information was obtained from the medical records. The tumours were classified into three subgroups as

Fig. 1 Sequence scheme. CA = contrast agent, VIBE = volume-interpolated breath-hold examination



follows: ER/PR+HER2– tumours and ER/PR+HER2+ tumours as luminal; ER/PR–HER2+ tumours as HER2-enriched; and ER/PR–/HER2– tumours as triple-negative [17, 18].

Image analysis

For data analysis, two radiologists (S.U.S. and N.C. with 5 and 17 years of experience, respectively) assessed conventional DCE-MRI in consensus. Morphological findings were described using BI-RADS MRI descriptors [19]. For conventional kinetic analysis, the region of interest (ROI) was manually placed on the most enhancing portion of the representative slice of the tumour at the pre-contrast, first post-contrast and last post-contrast images. The signal enhancement ratio (SER) of the tumour was defined as follows: $SER = (S_{1st} - S_{pre}) / (S_{last} - S_{pre})$, where S_{pre} , S_{1st} and S_{last} indicate the signal intensity on pre-contrast, first post-contrast and last post-contrast images, respectively [20].

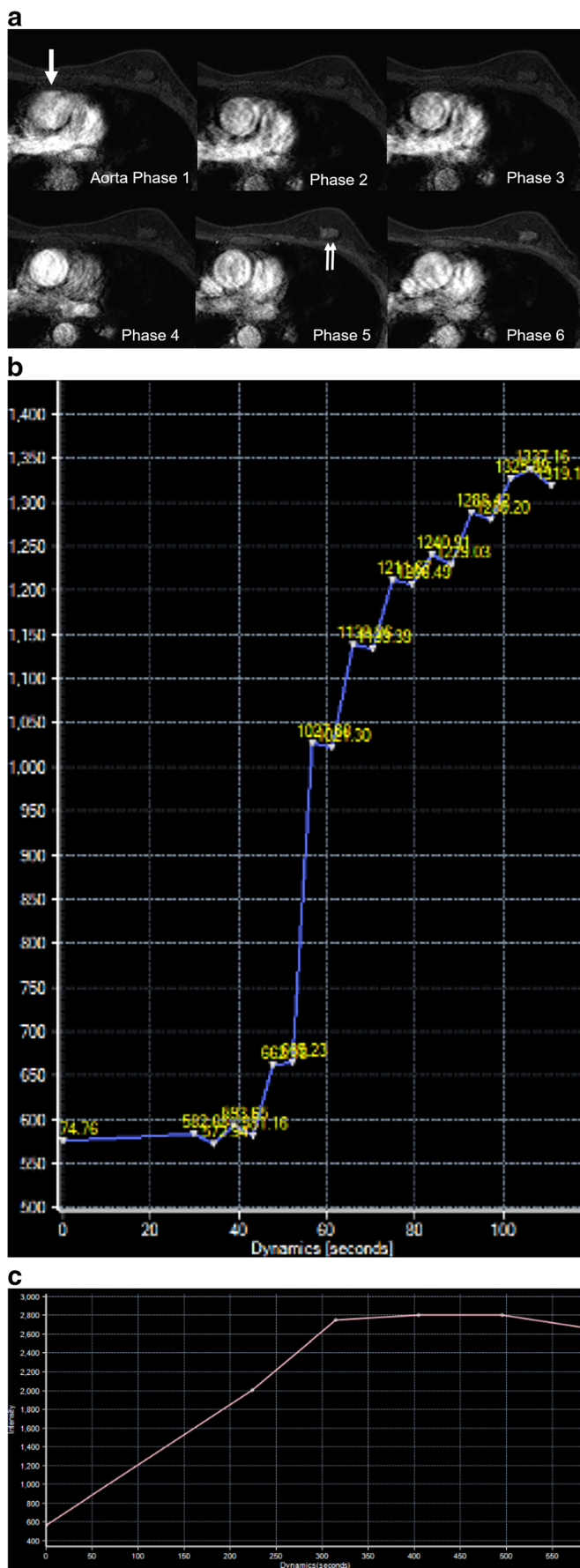
For ultrafast MRI, we analysed TTE and maximum slope (MS) of the tumour. The TTE was calculated as the phase of initial enhancement of the tumour relative to the ascending aorta, multiplied by the temporal resolution of each MRI, which was 3.8 s for TWIST-VIBE or 4.5 s for 4D TRAK-3D TFE [5, 8]. TTE was independently calculated by two radiologists (S.U.S. and N.C. with 5 and 17 years of experience, respectively). The reason why the aorta was set as a reference point was to minimise the effects of various circulation time and delayed contrast injection. We referred to the time point when the aorta began to become enhanced as phase 1 and to subsequent time points as phase 2, phase 3 and so on (Fig. 2, 3 and 4). The phase of the initial enhancement was defined as the first appearance of tumour enhancement on the post-contrast images. Tumour enhancement was identified when the signal intensity within the region of interest (ROI) in the tumour became more than 1.5 times the average signal intensity of the three unenhanced images within the same ROI. The ROI was manually placed over the most highly

Table 1 Acquisition parameters for conventional and ultrafast imaging

	Ultrafast—Siemens	Ultrafast—Philips	Conventional—Siemens	Conventional—Philips
Sequence	TWIST-VIBE	4D TRAK-3D TFE	VIBE	eTHRIVE
TR, ms	4.1	3.9 shortest	4.7	5.2 shortest
TE, ms	1.3	2.0 shortest	1.7	2.4 shortest
Flip angle, degree	10	12	10	12
Field of view, mm ²	320 × 320	300 × 300	320 × 320	300 × 300
Matrix size	288 × 259	320 × 320	384 × 384	332 × 332
In-plane resolution, mm	1.11 × 1.24	0.94 × 0.94	0.83 × 0.83	0.90 × 0.90
Slice thickness, mm	1.0	1.0	1.0	1.0
Voxel volume, mm ³	1.21	0.88	0.64	0.82
Phase resolution, %	90	100	100	100
Slice resolution, %	50		75	
Parallel imaging factor	CAIPIRINHA—5	SENSE—4 (phase direction), 2 (slice direction)	CAIPIRINHA—2	SENSE—3.2 (phase direction), 1 (slice direction)
Time resolution per volume, s	3.8	4.5	88	89
Total acquisition time, min	1:23	1:35	8:48	8:54

CAIPIRINHA = controlled aliasing in parallel imaging results in higher acceleration, eTHRIVE = enhanced T1-weighted high-resolution isotropic volume examination, SENSE = sensitivity encoding, TE = echo time, TFE = turbo field echo, TR = repetition time, TRAK = time-resolved MR angiography with keyhole, TWIST = time-resolved angiography with interleaved stochastic trajectories, VIBE = volume-interpolated breath-hold examination

Fig. 2 A 47-year-old woman with ductal carcinoma in situ (DCIS). **a** Ultrafast DCE-MRI shows an irregular enhanced mass in the left upper inner breast. The time-to-enhancement was 18 s, which was calculated as 4 (the interval from the initial enhancement of tumour [double arrows] relative to ascending aorta [arrow]) multiplied by 4.5 s. Surgical histopathology confirmed the mass as a 3.7-cm DCIS. **b** Time–intensity curve of ultrafast MRI shows a persistent initial rise at ultrafast MRI. **c** Time–intensity curve of conventional MRI shows a plateau pattern. The signal enhancement ratio was measured as 1.3



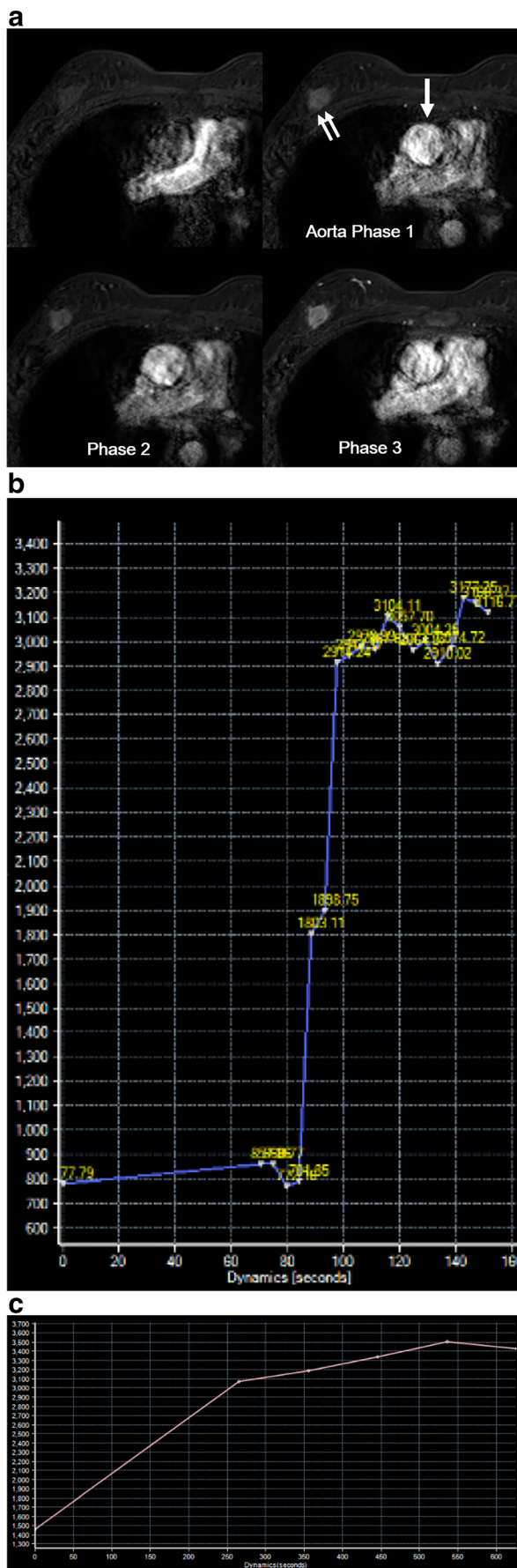


Fig. 3 A 52-year-old woman with invasive ductal carcinoma. **a** Ultrafast DCE-MRI shows an irregular enhanced mass in the right upper outer breast. The time-to-enhancement was 0 s because the timing of the initial enhancement of the tumour (double arrows) was the same as that of the ascending aorta (arrow). Surgical histopathology confirmed that the lesion was a 2.5-cm invasive ductal carcinoma with a histologic grade of 3 and Ki-67 level of 30%. **b** Time–intensity curve of ultrafast MRI shows a rapid initial rise. **c** Time–intensity curve of conventional MRI shows a plateau pattern. The signal enhancement ratio was measured as 1.1

enhanced portion of the tumour on the post-contrast ultrafast MRI. Then, the ROI was copied and pasted into the other phases of the ultrafast scans. The ROI size varied according to the size of the tumour. The mean ROI area was $15.9 \pm 12.0 \text{ mm}^2$ (range, 2.5–65.4 mm^2).

The MS was calculated from the maximal change of relative enhancement signal intensity between two time points, divided by their time difference [1/s] as performed in previous studies [1, 8] by using syngo.via and IntelliSpace Portal for Siemens Healthineers GmbH and Philips Healthcare, respectively.

Statistical analysis

The repeated measures ANOVA was performed to compare the median TTEs of two readers according to tumour size (> 2 vs. ≤ 2 cm), axillary LN metastasis (negative vs. positive), histologic grade (1 or 2 vs. 3), nuclear grade (1 or 2 vs. 3), ER status (positive vs. negative), PR status (positive vs. negative), HER2 status (positive vs. negative), level of Ki-67 (> 20 vs. $\leq 20\%$) and tumour subtype (luminal, HER2-enriched or triple-negative). To reduce type I error by multiple testing, Bonferroni correction was applied and $p < 0.005$ ($= 0.05/10$) was considered to be indicative of a significant difference. The Mann–Whitney U test and the Kruskal–Wallis H test were performed to compare the median MS and SER according to tumour size (> 2 vs. ≤ 2 cm), axillary LN metastasis (negative vs. positive), histologic grade (1 or 2 vs. 3), nuclear grade (1 or 2 vs. 3), ER status (positive vs. negative), PR status (positive vs. negative), HER2 status (positive vs. negative), level of Ki-67 (> 20 vs. $\leq 20\%$) and tumour subtype (luminal, HER2-enriched or triple-negative). We further analysed whether there were differences in TTE values between histopathologic features of tumours according to the two MRI machines. To determine the diagnostic accuracy for the prediction of the clinicopathological characteristics, the area under the receiver operating characteristic (ROC) curve (AUC), sensitivity and specificity were calculated. The optimal threshold for each discrimination was chosen at yielding the minimal value for $(1 - \text{sensitivity})^2 + (1 - \text{specificity})^2$ on the ROC curve [21]. For TTE calculation, intraclass correlation coefficient (ICC) was used to evaluate interobserver variability with the following qualitative interpretation: a value of 1.0 was considered perfect agreement; 0.81–0.99, almost perfect agreement;

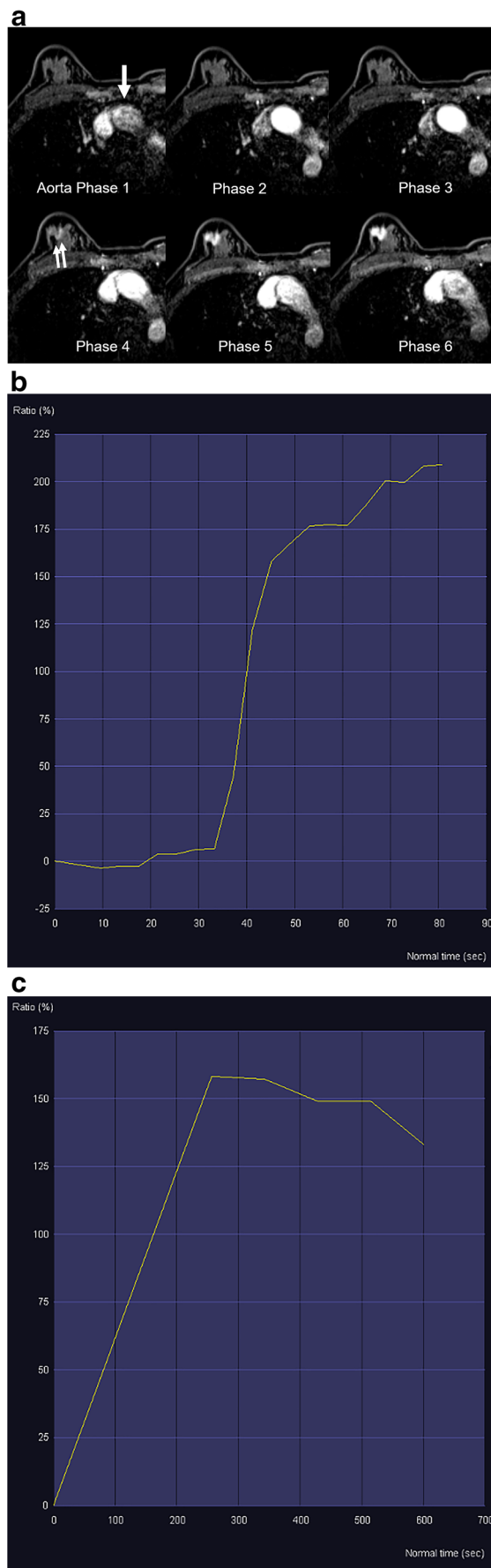


Fig. 4 A 53-year-old woman with invasive ductal carcinoma. **a** Ultrafast DCE-MRI shows an irregular enhanced mass in the right upper outer breast. The time-to-enhancement was 11.4 s, which was calculated as 3 (the interval from the initial enhancement of tumour [double arrows] relative to ascending aorta [arrow]) multiplied by 3.8 s. Surgical histopathology confirmed the lesion as a 1.6-cm invasive ductal carcinoma with a histologic grade of 2 and a Ki-67 level of 2%. **b** Time–intensity curve of ultrafast MRI shows a persistent initial rise. **c** Time–intensity curve of conventional MRI shows a washout pattern. The signal enhancement ratio was measured as 1.3

0.61–0.80, substantial agreement; 0.41–0.60, moderate agreement; 0.21–0.40, fair agreement; and 0.20 or less, slight agreement [22]. All statistical analyses were performed using MedCalc for Windows, version 19.1.3, MedCalc Software and Stata Statistical Software: Release 13, StataCorp LP, and $p < 0.05$ was considered to be indicative of a significant difference.

Results

Patients

With regard to the histopathology of the tumours, 86.9% (238/274) were invasive cancers, and 13.1% (36/274) were ductal carcinomas in situ (Table 2).

With regard to the MRI features, median lesion size, defined as the largest diameter of the tumour measured on MRI, was 2.2 cm (range, 0.5–9.5 cm), 85.4% (234/274) were masses and 14.6% (40/274) were non-mass enhancements (Table 3).

TTE according to pathologic characteristics

The median TTE of the invasive cancers was shorter than that of the in situ cancers (9.0 s [IQR 7.6, 11.4] vs. 9.0 s [IQR 9.0, 18.0] for reader 1, 9.0 s [IQR 9.0, 13.5] vs. 7.6 s [IQR 4.5, 9.0] for reader 2, $p < 0.001$) (Fig. 2) (Table 4). For the in situ cancers, there was no significant difference in TTE according to the tumour size, nuclear grade or hormonal receptor status. Of the invasive tumours, tumours > 2 cm had a shorter TTE than tumours ≤ 2 cm (9.0 s [IQR 7.6, 9.0] vs. 9.0 s [IQR 9.0, 13.5] for reader 1, 7.6 s [IQR 4.5, 9.0] vs. 9.0 s [IQR 4.5, 9.0] for reader 2, $p = 0.001$, Figs. 3 and 4). Tumours with a histologic grade 3 had a shorter TTE than tumours with a histologic grade 1 or 2 (9.0 s [IQR 7.6, 9.0] vs. 9.0 s [IQR 9.0, 11.4] for reader 1, 4.5 s [IQR 4.5, 9.0] vs. 9.0 s [IQR 4.5, 9.0] for reader 2, $p < 0.001$, Figs. 3 and 4). Tumours with a nuclear grade of 3 had a shorter TTE than tumours with a nuclear grade 1 or 2 (9.0 s [IQR 7.6, 9.0] vs. 9.0 s [IQR 9.0, 11.4] for reader 1, 4.5 s [IQR 4.5, 9.0] vs. 9.0 s [IQR 4.5, 9.0] for reader 2, $p < 0.001$). HER2-positive tumours had a shorter TTE than HER2-negative tumours (9.0 s [IQR 4.5, 9.0] vs. 9.0 s [IQR 7.6,

Table 2 Patient and tumour characteristics

Variable	Numbers
All cancers (<i>n</i> = 274)	
Invasive tumour size (cm)*	1.8 ± 1.4
≤ 2	178 (65.0)
> 2	96 (35.0)
Total tumour size, including in situ component (cm)*	3.1 ± 1.7
≤ 2	88 (32.1)
> 2	186 (67.9)
Invasive cancers (<i>n</i> = 238)	
Axillary lymph node metastasis	
Negative	183 (76.9)
Positive	55 (23.1)
Histologic grade	
1 or 2	179 (75.2)
3	59 (24.8)
Nuclear grade	
1 or 2	163 (68.5)
3	75 (31.5)
Oestrogen receptor	
Positive	196 (82.4)
Negative	42 (17.6)
Progesterone receptor	
Positive	158 (66.4)
Negative	80 (33.6)
HER2	
Positive	37 (15.5)
Negative	201 (84.5)
Level of Ki-67	
> 20%	14 (5.9)
≤ 20%	224 (94.1)
Subtype	
Luminal	198 (83.2)
HER2-enriched	14 (5.9)
Triple-negative	26 (10.9)

Note—Unless otherwise indicated, data are the number of patients with the percentage in parentheses

HER2 = human epidermal growth factor receptor 2

*Data are means ± standard deviation

11.4] for reader 1, 7.6 s [IQR 4.5, 9.0] vs. 9.0 s [IQR 4.5, 9.0] for reader 2, $p = 0.001$). The median TTE of tumours with high Ki-67 (> 20%) was shorter than that of tumours with low Ki-67 (≤ 20%) (6.1 s [IQR 3.8, 7.6] vs. 9.0 s [IQR 9.0, 11.4] for reader 1, 4.5 s [IQR 3.8, 9.0] vs. 7.6 s [IQR 4.5, 9.0] for reader 2, $p < 0.001$, Figs. 3 and 4). No differences were found in the median TTE according to the axillary LN status ($p = 0.031$) or ER positivity ($p = 0.019$), PR positivity ($p = 0.007$) or the immunohistochemical tumour subtype ($p = 0.275$). The ICC between two readers was 0.516, which indicates moderate agreement.

Table 3 MR imaging features of the 274 lesions

Characteristics	Malignant lesions (<i>n</i> = 274)
Median lesion size* on MRI (range) (cm)	2.2 (0.5–9.5)
MRI finding	
Mass	234 (85.4)
Shape	
Oval	9 (3.8)
Round	21 (9.0)
Irregular	204 (87.2)
Margin	
Circumscribed	19 (8.1)
Not circumscribed	
Irregular	177 (75.6)
Spiculated	38 (16.2)
Internal enhancement characteristics	
Homogeneous	14 (6.0)
Heterogeneous	177 (75.6)
Rim enhancement	43 (18.4)
Dark internal septations	0 (0)
Non-mass enhancement	40 (14.6)
Distribution	
Focal	1 (2.5)
Linear	1 (2.5)
Segmental	35 (87.5)
Regional	3 (7.5)
Internal enhancement patterns	
Homogeneous	3 (7.5)
Heterogeneous	24 (60.0)
Clumped	4 (10.0)
Clustered ring	9 (22.5)
BI-RADS assessment category	
4A	12
4B	20
4C	26
5	216

Note—Data are the numbers of lesions, and the values in parentheses are percentages

*It is the largest diameter of the lesion

With respect to the MRI machines, for data derived from Skyra machine, the median TTE was shorter in tumours > 20 mm (7.6 s [IQR 3.8, 7.6] vs. 11.4 s [IQR 7.6, 11.4], $p = 0.020$) or tumours with high histologic grade (7.6 s [IQR 3.8, 7.6] vs. 7.6 s [5.7, 11.4], $p = 0.049$). For data derived from Ingenia machine, the median TTE was shorter in invasive cancers (9.0 s [9.0, 9.0] vs. 9.0 s [IQR 9.0, 18.0], $p = 0.004$), tumours > 20 mm (9.0 s [IQR 9.0, 9.0] vs. 9.0 s [IQR 9.0, 18.0], $p = 0.007$) or tumours with high histologic (9.0 s [IQR 9.0, 9.0] vs. 9.0 s [IQR 9.0, 13.5], $p < 0.001$) or nuclear grade (9.0 s [IQR 9.0, 9.0] vs. 9.0 s [IQR 9.0, 13.5], $p < 0.001$), or

Table 4 Time-to-enhancement according to the histopathologic features of breast cancer lesions

		R1		R2		<i>p</i> value [†]
		Median (s)	IQR (s)	Median (s)	IQR (s)	
All cancer (<i>n</i> = 274)						
Invasiveness	In situ cancer (<i>n</i> = 36)	9.0	9.0, 18.0	9.0	9.0, 13.5	< 0.001
	Invasive cancer (<i>n</i> = 238)	9.0	7.6, 11.4	7.6	4.5, 9.0	
Invasive cancer (<i>n</i> = 238)						
Tumour size	≤ 20 mm (<i>n</i> = 77)	9.0	9.0, 13.5	9.0	4.5, 9.0	0.001
	> 20 mm (<i>n</i> = 161)	9.0	7.6, 9.0	7.6	4.5, 9.0	
Axillary LN metastasis	Negative (<i>n</i> = 183)	9.0	7.6, 9.0	7.6	4.5, 9.0	0.031
	Positive (<i>n</i> = 55)	9.0	9.0, 11.4	9.0	4.5, 9.0	
Histologic grade	1 or 2 (<i>n</i> = 179)	9.0	9.0, 11.4	9.0	4.5, 9.0	< 0.001
	3 (<i>n</i> = 59)	9.0	7.6, 9.0	4.5	4.5, 9.0	
Nuclear grade	1 or 2 (<i>n</i> = 163)	9.0	9.0, 11.4	9.0	4.5, 9.0	< 0.001
	3 (<i>n</i> = 75)	9.0	7.6, 9.0	4.5	4.5, 9.0	
Oestrogen receptor	Positive (<i>n</i> = 196)	9.0	7.6, 11.4	7.6	4.5, 9.0	0.019
	Negative (<i>n</i> = 42)	9.0	7.6, 9.0	4.5	4.5, 9.0	
Progesterone receptor	Positive (<i>n</i> = 158)	9.0	7.6, 11.4	9.0	4.5, 9.0	0.007
	Negative (<i>n</i> = 80)	9.0	7.6, 9.0	7.6	4.5, 9.0	
HER2	Positive (<i>n</i> = 37)	9.0	4.5, 9.0	7.6	4.5, 9.0	0.001
	Negative (<i>n</i> = 201)	9.0	7.6, 11.4	9.0	4.5, 9.0	
Ki-67	≤ 20% (<i>n</i> = 224)	9.0	9.0, 11.4	7.6	4.5, 9.0	< 0.001
	> 20% (<i>n</i> = 14)	6.1	3.8, 7.6	4.5	3.8, 9.0	
Subtype	Luminal (<i>n</i> = 198)	9.0	7.6, 11.4	7.6	4.5, 9.0	0.275
	HER2-enriched (<i>n</i> = 14)	9.0	9.0, 9.0	6.1	4.5, 9.0	
	Triple-negative (<i>n</i> = 26)	9.0	7.6, 9.0	4.5	4.5, 9.0	

HER2 = human epidermal growth factor receptor 2

[†] *p* value for non-parametric RM-ANOVA

tumours with ER negativity (9.0 s [IQR 9.0, 9.0] vs. 9.0 s [IQR 9.0, 13.5], *p* = 0.037) or PR negativity (9.0 s [IQR 9.0, 9.0] vs. 9.0 s [IQR 9.0, 13.5], *p* = 0.001), HER2 positivity (9.0 s [IQR 9.0, 9.0] vs. 9.0 s [IQR 9.0, 13.5], *p* = 0.018) and high Ki-67 level (4.5 s [IQR 0, 9.0] vs. 9.0 s [IQR 9.0, 9.0], *p* < 0.001) (Supplemental Table 1).

MS according to pathologic characteristics

No difference was found in the median MS values according to the tumour invasiveness (*p* = 0.730), tumour size (*p* = 0.190), axillary LN metastasis *p* = 0.176), histologic (*p* = 0.524) or nuclear grade (*p* = 0.239), ER positivity (*p* = 0.475), PR positivity (*p* = 0.877), HER2 positivity (*p* = 0.964), level of Ki-67 (*p* = 0.282) and tumour subtype (*p* = 0.642) (Supplemental Table 2).

SER of conventional DCE-MRI according to pathologic characteristics

No difference was found in the median SER values according to the tumour invasiveness (*p* = 0.163), tumour size (*p* = 0.467), axillary LN metastasis (*p* = 0.091), histologic grade

(*p* = 0.360), nuclear grade (*p* = 0.753), ER positivity (*p* = 0.311), PR positivity (*p* = 0.797), HER2 positivity (*p* = 0.754), level of Ki-67 (*p* = 0.746) and tumour subtype (*p* = 0.351).

ROC analysis

Areas under the ROC curves (*Az*) and cut-off values for each predictor are presented in Supplemental Table 3. For reader 1, analyses of ROC curves showed that TTEs can moderately predict tumour invasiveness (*Az* = 0.647, *p* = 0.001), tumour size (*Az* = 0.597, *p* = 0.010), histologic grade (*Az* = 0.662, *p* < 0.001), nuclear grade (*Az* = 0.631, *p* < 0.001), ER negativity (*Az* = 0.590, *p* = 0.028), PR negativity (*Az* = 0.584, *p* = 0.019), HER2 positivity (*Az* = 0.605, *p* = 0.030) and level of Ki-67 (*Az* = 0.822, *p* < 0.001). The cut-off values for predicting invasiveness, tumour size, histologic grade, nuclear grade or ER negativity were all 9.0 s. The cut-off values for prediction of PR negativity, HER2 positivity and level of Ki-67 were 11.4, 3.8 and 7.6 s, respectively. For reader 2, analyses of ROC curves showed that TTEs can moderately predict tumour invasiveness (*Az* = 0.772, *p* < 0.001), tumour size (*Az* = 0.575, *p* = 0.053), histologic grade (*Az* = 0.623, *p* =

0.002), nuclear grade ($A = 0.632$, $p < 0.001$), ER negativity ($Az = 0.571$, $p = 0.143$), PR negativity ($Az = 0.566$, $p = 0.092$), HER2 positivity ($Az = 0.594$, $p = 0.033$) and level of Ki-67 ($Az = 0.660$, $p = 0.055$). The cut-off values for predicting invasiveness or HER2 positivity were 7.6 s. The cut-off values for histologic grade or nuclear grade were 4.5 s.

Discussion

In our study, we found that the mean TTE of invasive breast cancers or aggressive tumours in ultrafast MRI was shorter than that of in situ cancer or less aggressive tumours, respectively. It is known that histopathologic features such as large tumour size, axillary lymph nodal metastasis, high histologic or nuclear grade, ER or PR negativity, HER2 positivity and high Ki-67 level are associated with aggressive tumour. Our results are in line with those of previous studies in which lesions showing rapid early enhancement kinetic parameters derived from conventional DCE-MRI were correlated with biologically aggressive tumours or tumours with a high histologic grade [9–12]. There have been many publications regarding the correlations between various MRI parameters and prognostic factors or survival outcomes for patients with breast tumours (Supplemental Table 4) [13, 14]. Using pharmacokinetic modelling, a high $K(\text{trans})$ has been shown to correlate with high histologic grade, high Ki-67 level or hormonal receptor negativity [23, 24]. The notable finding of our study lies in the usage of very early kinetic parameters derived from ultrafast DCE-MRI.

Using ultrafast DCE-MRI, a recent study by Goto et al found that tumours of a high grade, hormonal receptor negativity and high Ki-67 level showed a short TTE and larger MS [8]. In regard to TTE, the results are similar to our results. In addition, the median TTE (9.9 s) of malignant tumours in Goto's study is similar to the median TTE (9.0 s) of invasive cancers in our study. However, contrary to their results, we could not find significant differences in MS according to the histopathologic features.

An interesting result of our study is that the potential of very early kinetic parameters in our study is consistent with other study results. The initial enhancement ratio, defined as the mean percentage increase of the signal between the pre-contrast and the first post-contrast DCE-MRI series, has been shown to be associated with invasive disease [15, 16], high histologic grade [15, 16], node positivity [16], high Ki-67 [16] and tumour subtype [16]. In the study, the diagnostic utility of the initial enhancement ratio was compared to that of the washout kinetic analysis. The authors found that the initial enhancement ratio showed better diagnostic utility for positive axillary nodes and similar utility for invasive cancer and high Ki-67 than the washout kinetic analysis [16]. Thus, these studies have consistently suggested that wash-in temporal kinetic

information could alternatively provide prognostic information instead of washout curve analysis performed in conventional DCE-MRI. In line with these studies, SER derived from conventional DCE-MRI in our study population did not show any differences according to the histopathologic features, contrary to TTE derived from ultrafast MRI. This might be because our conventional DCE-MRI scans were scanned at delayed phase. In addition, AUCs for the TTE at ultrafast MRI to predict clinicopathologic features ranged from 0.556 to 0.822, which indicates that the TTE at ultrafast MRI alone is not adequate for clinical decision-making. In addition, very early kinetic information from ultrafast breast MRI would be integrated into the abbreviated breast MRI protocol in the future. The concept of an abbreviated MRI protocol composed of one pre- and one post-contrast T1-weighted MRI sequence has been shown to make breast MRI more feasible while maintaining the equivalent diagnostic accuracy in a screening setting [15, 25–28]. However, for characterising lesions, the performance of the abbreviated MRI is inferior to that of a full diagnostic MRI [15, 25–28]. This might be due to a lack of delayed kinetic information. The feasibility of combining abbreviated MRI with ultrafast DCE-MRI in the specific prognostic task should also be investigated.

The shorter TTE found in invasive breast cancers or aggressive tumours in our study could probably be explained by the fact that aggressive tumours have high neovascularisation [29] of immature vasculature with increased permeability. The initial slope in ultrafast DCE-MRI has been shown to correlate with microvessel density in invasive breast cancer [20]. These vasculature characteristics may increase the rate at which the contrast agent enters or exits the vessels. Based on our results that biologically relevant parameters are derived from the very early kinetics of ultrafast DCE-MRI, we suggest that ultrafast DCE-MRI should be added to the abbreviated MRI for clinical usage. Applying the inflow dynamic information to an abbreviated MRI could potentially provide kinetic information, which can be used as an alternative to delayed kinetic information while maintaining a short MRI acquisition time. A recent study has also reported that the addition of ultrafast MRI to abbreviated MRI improves specificity, mainly in correctly reclassifying benign masses, without decreasing sensitivity and while maintaining the short interpretation and acquisition times [30].

With regard to the acceleration technique for ultrafast MRI, the view-sharing technique was used for our study. Full k-space sampling was performed only once for the non-contrast images, and the centre of the k-space was sampled more frequently than the periphery; this was because only the brightness and darkness changes after the gadolinium injection and the centre of the k-space contained brightness and darkness information, and the outer part contained spatial resolution and edge information [31]. Subsequently, the data from the different partial k-space samplings were combined to create a series of images. Thus, ultrafast DCE-MRI has not

been considered adequate for quantitative analysis. However, based on the significant associations between TTE from ultrafast MRI and the prognostic factors in our study, we can infer that the quantitative analysis of ultrafast MRI using the view-sharing technique might be feasible in future studies.

Our study has several limitations. First, this study was a single-centre retrospective analysis, which limits the generalisability of the study results. Second, this study was performed using 3 T scanners from two vendors. The detailed parameters and values are different because the scanners do not use the same scan techniques or protocols. To evaluate the possibility of TTE as an imaging biomarker, the lack of normalisation or standardisation procedure might be one of the major limitations. However, shorter median TTE observed in tumours > 20 mm or tumours with high histologic grade compared to that of their counterparts were consistently found regardless of vendor differences. Small data sample size from Skyra machine might be the reason for inconsistent results regarding tumours with ER or PR negativity, HER2 positivity and high Ki-67 level. Third, the assessment of TTE was qualitatively evaluated, and thus, the time intervals less than the temporal resolution (3.8 or 4.5 s) could not be detected, resulting in coarse estimation of TTE. Even though interobserver variability was moderate, visual assessment of the most highly enhanced portion and manual placement of ROI might have affected the value of TTE. In addition, the TTE values may depend on many technical parameters, such as the contrast dosage and specific scan protocol settings, and these parameters need to be further clarified in future studies.

In conclusion, ultrafast DCE-MRI shows that the TTE is shorter in invasive cancer or aggressive tumours than in in situ cancer or less aggressive tumours. When ultrafast DCE-MRI is added to the abbreviated MRI, the added early kinetic information can provide biologically relevant information instead of delayed kinetics on conventional MRI.

Funding information This study has received funding by a grant (no. 04-2017-0470) from the Seoul National University Hospital Research Fund.

Compliance with ethical standards

Guarantor The scientific guarantor of this publication is Nariya Cho MD, PhD, Professor of the Department of Radiology, Seoul National University Hospital.

Conflict of interest The authors declare that they have no conflict of interest.

Statistics and biometry No complex statistical methods were necessary for this paper.

Informed consent Written informed consent was waived by the Institutional Review Board.

Ethical approval Institutional Review Board approval was obtained.

Methodology

- Retrospective
- Observational
- Performed at one institution

References

1. Mann RM, Mus RD, van Zelst J, Geppert C, Karssemeijer N, Platel B (2014) A novel approach to contrast-enhanced breast magnetic resonance imaging for screening: high-resolution ultrafast dynamic imaging. *Invest Radiol* 49:579–585
2. Herrmann KH, Baltzer PA, Dietzel M et al (2011) Resolving arterial phase and temporal enhancement characteristics in DCE MRM at high spatial resolution with TWIST acquisition. *J Magn Reson Imaging* 34:973–982
3. Pineda FD, Medved M, Wang S et al (2016) Ultrafast bilateral DCE-MRI of the breast with conventional Fourier sampling: preliminary evaluation of semi-quantitative analysis. *Acad Radiol* 23: 1137–1144
4. Platel B, Mus R, Welte T, Karssemeijer N, Mann R (2014) Automated characterization of breast lesions imaged with an ultrafast DCE-MR protocol. *IEEE Trans Med Imaging* 33:225–232
5. Mus RD, Borelli C, Bult P et al (2017) Time to enhancement derived from ultrafast breast MRI as a novel parameter to discriminate benign from malignant breast lesions. *Eur J Radiol* 89:90–96
6. Abe H, Mori N, Tsuchiya K et al (2016) Kinetic analysis of benign and malignant breast lesions with ultrafast dynamic contrast-enhanced MRI: comparison with standard kinetic assessment. *AJR Am J Roentgenol* 207:1159–1166
7. Onishi N, Sadinski M, Gibbs P et al (2019) Differentiation between subcentimeter carcinomas and benign lesions using kinetic parameters derived from ultrafast dynamic contrast-enhanced breast MRI. *Eur Radiol*. <https://doi.org/10.1007/s00330-019-06392-5>
8. Goto M, Sakai K, Yokota H et al (2019) Diagnostic performance of initial enhancement analysis using ultra-fast dynamic contrast-enhanced MRI for breast lesions. *Eur Radiol* 29:1164–1174
9. Szabo BK, Aspelin P, Kristoffersen Wiberg M, Tot T, Bone B (2003) Invasive breast cancer: correlation of dynamic MR features with prognostic factors. *Eur Radiol* 13:2425–2435
10. Tuncbilek N, Karakas HM, Okten OO (2005) Dynamic magnetic resonance imaging in determining histopathological prognostic factors of invasive breast cancers. *Eur J Radiol* 53:199–205
11. Baltzer PA, Vag T, Dietzel M et al (2010) Computer-aided interpretation of dynamic magnetic resonance imaging reflects histopathology of invasive breast cancer. *Eur Radiol* 20:1563–1571
12. Leong LC, Gombos EC, Jagadeesan J, Fook-Chong SM (2015) MRI kinetics with volumetric analysis in correlation with hormonal receptor subtypes and histologic grade of invasive breast cancers. *AJR Am J Roentgenol* 204:W348–W356
13. Nam SY, Ko ES, Lim Y et al (2018) Preoperative dynamic breast magnetic resonance imaging kinetic features using computer-aided diagnosis: association with survival outcome and tumor aggressiveness in patients with invasive breast cancer. *PLoS One* 13: e0195756
14. Kim JJ, Kim JY, Kang HJ et al (2017) Computer-aided diagnosis-generated kinetic features of breast cancer at preoperative MR imaging: association with disease-free survival of patients with primary operable invasive breast cancer. *Radiology* 284:45–54
15. Heacock L, Melsaether AN, Heller SL et al (2016) Evaluation of a known breast cancer using an abbreviated breast MRI protocol: correlation of imaging characteristics and pathology with lesion detection and conspicuity. *Eur J Radiol* 85:815–823

16. Heacock L, Lewin AA, Gao Y et al (2018) Feasibility analysis of early temporal kinetics as a surrogate marker for breast tumor type, grade, and aggressiveness. *J Magn Reson Imaging* 47:1692–1700
17. Perou CM, Sorlie T, Eisen MB et al (2000) Molecular portraits of human breast tumours. *Nature* 406:747–752
18. Wolff AC, Hammond ME, Hicks DG et al (2013) Recommendations for human epidermal growth factor receptor 2 testing in breast cancer: American Society of Clinical Oncology/College of American Pathologists clinical practice guideline update. *J Clin Oncol* 31:3997–4013
19. Morris EA, Comstock CE, Lee CH et al (2013) ACR BI-RADS® magnetic resonance imaging. In: ACR BI-RADS® atlas, breast imaging reporting and data system. American College of Radiology, Reston
20. Mori N, Abe H, Mugikura S et al (2018) Ultrafast dynamic contrast-enhanced breast MRI: kinetic curve assessment using empirical mathematical model validated with histological microvessel density. *Acad Radiol*. <https://doi.org/10.1016/j.acra.2018.08.016>
21. Youden WJ (1950) Index for rating diagnostic tests. *Cancer* 3:32–35
22. Landis JR, Koch GG (1977) The measurement of observer agreement for categorical data. *Biometrics* 33:159–174
23. Koo HR, Cho N, Song IC et al (2012) Correlation of perfusion parameters on dynamic contrast-enhanced MRI with prognostic factors and subtypes of breast cancers. *J Magn Reson Imaging* 36:145–151
24. Kim JY, Kim SH, Kim YJ et al (2015) Enhancement parameters on dynamic contrast enhanced breast MRI: do they correlate with prognostic factors and subtypes of breast cancers? *Magn Reson Imaging* 33:72–80
25. Grimm LJ, Soo MS, Yoon S, Kim C, Ghate SV, Johnson KS (2015) Abbreviated screening protocol for breast MRI: a feasibility study. *Acad Radiol* 22:1157–1162
26. Kuhl CK, Schrading S, Strobel K, Schild HH, Hilgers RD, Bieling HB (2014) Abbreviated breast magnetic resonance imaging (MRI): first postcontrast subtracted images and maximum-intensity projection—a novel approach to breast cancer screening with MRI. *J Clin Oncol* 32:2304–2310
27. Mango VL, Morris EA, David Dershaw D et al (2015) Abbreviated protocol for breast MRI: are multiple sequences needed for cancer detection? *Eur J Radiol* 84:65–70
28. Sheth D, Abe H (2017) Abbreviated MRI and accelerated MRI for screening and diagnosis of breast cancer. *Top Magn Reson Imaging* 26:183–189
29. Su MY, Cheung YC, Fruehauf JP et al (2003) Correlation of dynamic contrast enhancement MRI parameters with microvessel density and VEGF for assessment of angiogenesis in breast cancer. *J Magn Reson Imaging* 18:467–477
30. Oldrini G, Fedida B, Poujol J et al (2017) Abbreviated breast magnetic resonance protocol: value of high-resolution temporal dynamic sequence to improve lesion characterization. *Eur J Radiol* 95:177–185
31. Song T, Laine AF, Chen Q et al (2009) Optimal k-space sampling for dynamic contrast-enhanced MRI with an application to MR renography. *Magn Reson Med* 61:1242–1248

Publisher's note Springer Nature remains neutral with regard to jurisdictional claims in published maps and institutional affiliations.